Demonstration of Staggered Ambiguous SAR Mode for Ship Monitoring Using TerraSAR-X

Nertjana Ustalli
Microwaves and Radar Institute
German Aerospace Center (DLR)
Weßling, Germany
nertjana.ustalli@dlr.de

Maxwell Nogueira Peixoto
Microwaves and Radar Institute
German Aerospace Center (DLR)
Weßling, Germany
maxwell.nogueirapeixoto@dlr.de

Thomas Kraus
Microwaves and Radar Institute
German Aerospace Center (DLR)
Weßling, Germany
T.Kraus@dlr.de

Ulrich Steinbrecher
Microwaves and Radar Institute
German Aerospace Center (DLR)
Weßling, Germany
Ulrich.Steinbrecher@dlr.de

Gerhard Krieger
Microwaves and Radar Institute
German Aerospace Center (DLR)
Weßling, Germany
gerhard.krieger@dlr.de

Michelangelo Villano
Microwaves and Radar Institute
German Aerospace Center (DLR)
Weßling, Germany
michelangelo.villano@dlr.de

***Abstract*—Maritime surveillance employing synthetic aperture radar (SAR) necessitates the simultaneous achievement of a wide swath and high resolution, enabling effective monitoring of vast areas with enhanced detection capabilities. However, conventional SAR modes encounter limitations as widening the swath compromises azimuth resolution. Ambiguous SAR modes, such as the staggered ambiguous mode utilizing continuous variation of short pulse repetition intervals and low pulse repetition frequency mode, surmount this constraint by enabling the imaging of a wide swath with high resolution. Both modes ensure remarkable detection performance even for small ships without relying on digital beamforming or multiple receive apertures. This paper presents the demonstration of the staggered ambiguous mode through experimental data acquired by the TerraSAR-X satellite over the North Sea. Despite technical limitations inherent in the SAR instrument, a swath of 110 km was successfully imaged with an azimuth resolution of 2.2 m. A probability of detection greater than 0.8 was achieved for small ships measuring 21 m × 6 m. Range ambiguities of the ships were identified based on their characteristics and position, and subsequently rejected. The detected ships were validated with maritime positioning data obtained from their automatic identification system. These findings provide compelling evidence and rationale for adopting the ambiguous SAR modes in current and future SAR systems and missions.**

Keywords—Ambiguities, automatic identification system (AIS), high-resolution wide-swath imaging, maritime monitoring, ship detection, synthetic aperture radar (SAR), staggered SAR, TerraSAR-X

I. Introduction

Synthetic aperture radar (SAR) images have great potential for observing and monitoring the maritime environment, benefiting applications like maritime traffic control, pollution monitoring, fisheries, smuggling prevention, and defense purposes. User requirements include persistence, high detection performance, and responsiveness. Mapping wider swaths improves observation frequency, while higher resolution SAR images enhance detection performance by providing more favorable statistics. On-board processing reduces latency for improved responsiveness.

However, wide-swath coverage and high-resolution imaging pose contradicting requirements on the pulse repetition frequency (PRF). Controlling range ambiguities requires a pulse repetition interval (PRI) greater than the time needed to collect returns from the entire illuminated swath. A large PRI (low PRF) limits unambiguous Doppler bandwidth and therefore the achievable azimuth resolution if azimuth ambiguities have to be controlled [1]. A wide swath can also be mapped with ScanSAR or TOPS (Terrain Observation by Progressive Scans), but the azimuth resolution is still impaired. Digital beamforming (DBF) and multiple aperture recording are promising techniques that overcome these limitations and achieve high-resolution wide-swath images, but also imply higher system complexity and costs. Furthermore, the use of co-prime SAR concepts allows for reducing the number of transmitted pulses and the data rate. Azimuth ambiguities of ships are then discriminated by comparing two distinct SAR images generated from the original data set [2], [3].

In [4], we have proposed two high-resolution wide-swath ship monitoring modes that "tolerate" ambiguities: low PRF and staggered (high PRF) ambiguous modes. Both map wide swaths by using a wide elevation beam on both transmit and receive obtained through tapering [5]. The low PRF mode collects echoes from the wide swath with a PRF smaller than the nominal Doppler bandwidth, achieving high azimuth resolution by processing the full Doppler bandwidth. The staggered ambiguous mode uses a sequence of distinct PRIs with a mean PRF greater than the Doppler bandwidth. An even larger swath, but with a reduced azimuth resolution, can be obtained with a ScanSAR mode that tolerates azimuth ambiguities, as proposed by NovaSAR [6].

The staggered ambiguous mode in [4] and the staggered SAR system employing DBF techniques [7] - [10] exhibit notable differences. In both systems, a wide elevation transmit beam illuminates a wide swath, and the radar echo corresponding to each transmitted pulse returns with increasing delays as the elevation angle (and slant range) increases. However, in staggered SAR, DBF is utilized on the receive side to steer a narrow high-gain beam towards the direction of arrival (DoA) of the ground echo, exploiting the one-to-one relationship between the radar pulse travel time and its DoA. As different beams receive echoes from distinct pulses, there is no overlap among them. The received echoes from various beams are rearranged, ensuring that the returns from a stationary ship align at the same slant range across all range lines. Due to the radar's inability to receive while transmitting, some "blind areas" will be present on the received data. As the PRI is continuously varied, the locations of the blind areas will be different for each range line, as they are related to the time distances between the transmitted pulses.

In the staggered ambiguous mode, the same wide elevation transmit beam is also used to receive the radar echoes. In this case, the receive echo window, i.e., the time interval during which the receiver is turned on and can receive radar echoes, is typically much shorter than the duration of the radar echo from the illuminated swath. As a result, preceding and succeeding echoes arrive at the radar at the same time as the desired return, resulting in range ambiguities. Unlike in SAR modes with constant PRI, where range ambiguous echoes of a scatterer appear at the same ranges along the entire synthetic aperture, range ambiguities in the staggered mode are located at different ranges for different range lines, as the time difference between the transmit pulses continuously varies. After SAR processing, the ambiguous energy is thus incoherently integrated and spread almost uniformly across the Doppler spectrum [9], [11]. This leads to two effects: first, the presence of range ambiguities of ships within the imaged swath, and second, an increased level of sea clutter, which must be considered when assessing detection performance. We have shown in [4] that the ambiguous SAR modes allows detecting small ships, i.e., of 21 m × 6 m size, with a probability of detection of 0.97 and a false alarm rate of 1.26×10^{-7}. The ambiguous modes therefore achieve a swath similar to that of a ScanSAR mode and a resolution cell of 2 m^2, similar to that of a spotlight mode. For a ScanSAR mode that images the same swath with a coarser resolution, the probability of detection would be less than 0.3, i.e., about 70% of the ships would be missed, assuming the same ship size and false alarms as in the ambiguous modes.

This paper presents the design of an experimental TerraSAR-X acquisition using the high-resolution wide-swath staggered (high PRF) ambiguous mode for ship monitoring, the analysis of the expected performance, the processing of the data, and the validation of the results.

II. TerraSAR-X Experiment: Parameter Selection and Expected Performance

TerraSAR-X is a conventional phased-array SAR that can be operated in staggered SAR mode, because it has 512 different PRIs and can be commanded to transmit pulses based on a sequence of M distinct PRIs that then repeats periodically, as demonstrated in [9].

A. Parameter selection

As test site for the demonstration has been chosen an area in the North Sea not far from the German Bight. The imaged point closest to the coast has been selected to be approximately 27 km away from the Dutch coast, in order to avoid range ambiguities caused by strong land scatterers that could interfere with the ship detection. Fig. 1 shows the test site; the red rectangle delimits the area of the acquired SAR image.

The selected elevation beam illuminates a 110 km ground swath with minimum and maximum look angles of 53.74° and 56.67°, respectively. High incidence angles are selected because the sea clutter return is expected to be lower than at lower incidence angles. Moreover, the 110 km ground swath is not defined by the 3 dB antenna beamwidth, but by a beamwidth corresponding to about 8 dB below the maximum, as TerraSAR-X still provides adequate noise equivalent sigma zero (NESZ), i.e., adequate signal-to-noise ratio (SNR), ensuring high ship detection performance over this wide swath, as discussed in Section II.B.

Once the beam has been selected, other system parameters such as the PRI sequence, the pulse length τ, and the chirp bandwidth B_r, must be chosen to ensure the best ship detection performance while respecting the TerraSAR-X technological constraints. We have shown in [4] that the best detection performance for an X-band system is obtained for the highest possible duty cycle value because it implies a better NESZ (or SNR) and for the highest selectable chirp bandwidth, because the effect of the improved resolution overcomes that of the reduced NESZ. The main TerraSAR-X parameters and constraints to be considered for the experiment are summarized in Table I.

One of the constraints is the maximum duty cycle D_{max} of 20%, defined as the ratio of the uncompressed pulse length τ to the PRI, which should hold for each distinct PRI and therefore also for the shortest PRI_{min}:

$$PRI_{min} \geq \frac{\tau}{D_{max}}. \tag{1}$$

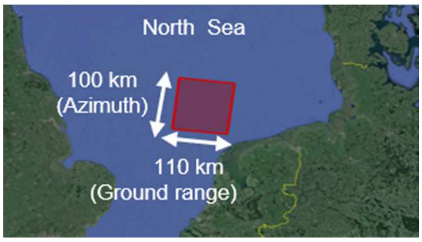

Fig. 1 North Sea test site near the German Bight selected for the experimental acquisition in staggered ambiguous mode. The red rectangle delimits the area of the acquired SAR image.

Table I Main TerraSAR-X parameters and constraints to be considered for the experiment.

Parameter	Symbol	Value
Radar wavelength	λ	0.0311 m
Orbit height	h	515 km
Antenna size	$L_a \times W_a$	4.8 m × 0.7 m
Maximum duty cycle	D_{max}	20%
Maximum echo window length	EWL_{max}	32768 samples
Maximum pulse length	τ_{max}	67 µs
Minimum pulse length	τ_{min}	15 µs
Time guard between receive and transmit	τ_{RX-TX}	5.2 µs
Time guard between transmit and receive	τ_{TX-RX}	3.271 µs
Sampling frequency	F_r	$1.1\times B_r$
Minimum selectable pulse repetition frequency	$PRF_{min_{TS-X}}$	1999.96 Hz
Maximum selectable pulse repetition frequency	$PRF_{max_{TS-X}}$	6706.91 Hz

Another constraint is the maximum receive echo window length EWL_{max}, i.e., the maximum number of samples that can be memorized in the TerraSAR-X buffer, which is 32768 samples. This constraint should hold for each distinct PRI and therefore also for the longest PRI_{max}:

$$PRI_{max} \leq \frac{EWL_{max}}{F_r} + \tau + \tau_{RX-TX} + \tau_{TX-RX} \, , \qquad (2)$$

where τ_{RX-TX} and τ_{TX-RX} are the time guards between receive and transmit and transmit and receive, respectively (see Table I), F_r is the sampling frequency that for TerraSAR-X is approximately 10% higher than the selected chirp bandwidth B_r.

A chirp bandwidth of 300 MHz, the highest available in TerraSAR-X which allows for the highest range resolution, cannot be chosen for this experiment. The maximum duty cycle constraint of (1), in fact, requires τ < 41.3 µs. By substituting the values of the maximum echo window length and the guard times from Table I in (2), it turns out that for values of τ < 41.3 µs, PRI_{max} is smaller than the minimum selectable PRI value for TerraSAR-X. While for a 150 MHz chirp bandwidth it is possible to find a sequence of PRIs that satisfies both constraints (1) and (2) for a pulse length of 30 µs, the data rate from the instrument buffer to the mass memory imposes a further limitation on the chirp bandwidth for such a large swath. A chirp bandwidth of 100 MHz has therefore been chosen for this experiment, resulting in a ground range resolution at near range R_{min} of 1.72 m, if no windows are used within the processing. For a pulse length of 45 µs, is it possible to design a sequence of M = 43 PRIs (selected among the 512 available PRIs) that satisfies both constraints in (1) and (2) and follows an almost linear decreasing trend. The mean PRF of sequence, which is the reciprocal of the mean PRI, is PRF_{mean} = 3525 Hz, which is greater than the 3 dB Doppler bandwidth of the system, B_{Dop} = 2807 Hz. The average duty cycle of the sequence is 16.1 %. Table II reports the selected parameters for the experiment.

Because TerraSAR-X has a limited number of selectable PRFs, the condition that two consecutive azimuth samples are never missed [8] is not satisfied for each range line for the selected PRI sequence. This usually allows for more accurate interpolation of non-uniformly sampled raw data on a uniform grid and lower azimuth ambiguity-to-signal ratios, but is not a strict requirement and can be tolerated for this mode, where range ambiguities dominate over azimuth ambiguities.

Table II Selected parameters for the experiment.

Parameter	Symbol	Value
Wave polarization		HH
Minimum slant range	R_{min}	948.7 km
Maximum slant range	R_{max}	1047.1 km
Chirp bandwidth	B_r	100 MHz
Pulse length	τ	45 µs
Mean PRF	PRF_{mean}	3525 Hz

B. *Expected performance*

The detection performance ultimately depends on the ship size and the statistics of the background disturbance, which includes the sea clutter and the thermal noise. Furthermore, the specific ambiguous mode requires careful consideration of the effects of ambiguities of both the sea clutter, which might be significantly amplified, and of the ships, which might result in false alarms.

As for the thermal noise, the NESZ is evaluated for the selected antenna beam and shown as a function of ground range in Fig. 2 (see black curve). The NESZ ranges from -14 dB at the swath center to about -4 dB at near and far range and is much worse than for typical TerraSAR-X stripmap acquisitions.

The sea clutter will be amplified in the ambiguous mode by a factor given by one plus the integrated ambiguity-to-signal ratio of the system, that should account for both range and azimuth ambiguities. This amplification occurs because the unambiguous sea clutter component and the ambiguous sea clutter components are independent of each other, as they originate from different areas. The range ambiguity-to-signal ratio (RASR) for a variable PRI SAR is evaluated using the closed form expression in [9] for a backscatter trend constant over range. It is shown in Fig. 3 as a function of the ground range, and ranges from -4.8 dB at the swath center to 8.8 dB at far range. The azimuth ambiguity-to-signal ratio (AASR) for a variable PRI SAR is also evaluated following the approach in [9], i.e., as the difference of the integrated side lobe ratios and is in the order of -11.5 dB, therefore negligible compared to the RASR. Consequently, we can approximate the total sea clutter as the sea clutter of the unambiguous component multiplied by one plus the RASR.

The backscatter level of the sea clutter depends on the condition of the sea. Typical mean values of the backscatter in X band for calm sea range between -16 and -18 dB, but a more conservative value of -14 dB could also be considered to account for the increase of backscatter due to wind. Fig. 2 compares the total background disturbance for backscatter levels of the sea clutter of -14, -16, and -18 dB (represented by the blue, red and green curves) with the NESZ (represented by the black curve).

Finally, the probability of detection of a small ship of 21 m × 6 m size is evaluated using the closed form expression in [12] and [4] for 1000 false alarms per million of km^2, corresponding to a false alarm rate of 1.26×10^{-7}, the total disturbance of Fig. 2 and an azimuth resolution of 2.2 m. Due to the variable PRI operation, which results in an incoherent integration of the ambiguous echoes appearing at different ranges, the disturbance resulting from the ambiguous clutter can be considered as noise-like. The probability of detection is shown in Fig. 4 as a function of ground range for different backscatter levels of the sea clutter. The achieved probability of detection is always better than 0.5 for a backscatter level of the sea clutter of -14 dB. The performance of Fig. 4 does not account for the false alarms due to the ambiguities of ships.

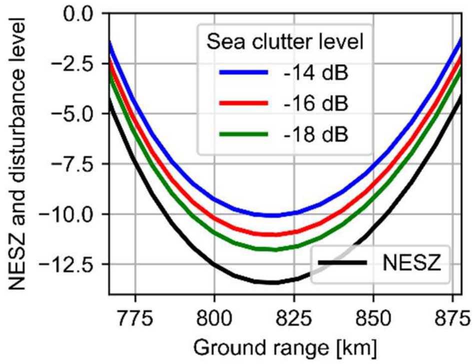

Fig. 2 NESZ and total disturbance as a function of the ground range for the selected antenna beam and the parameters of Table II.

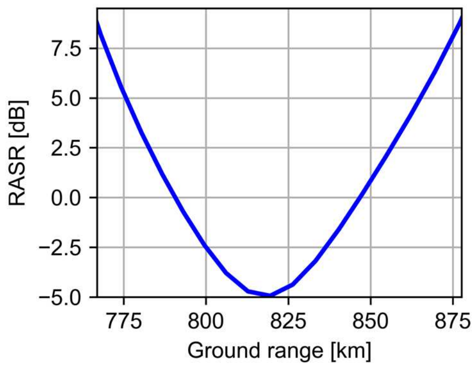

Fig. 3 RASR as a function of the ground range for the selected antenna beam and the parameters of Table II.

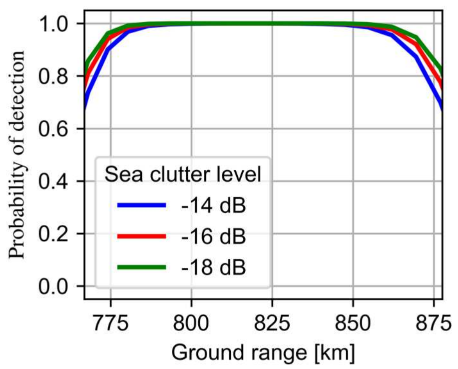

Fig. 4 Probability of detection of a small ship of 21 m × 6 m size as a function of ground range for 1000 false alarms per million of km^2, corresponding to a false alarm rate of 1.26×10^{-7} and different backscatter levels of the sea clutter.

III. Data Processing

The TerraSAR-X experimental acquisition in staggered ambiguous mode has been performed on July 11, 2022 over the North Sea. The sequence of 43 PRIs is repeated 1200 times. The echoes, received by the radar between consecutive transmitted pulses, have different duration, as different PRIs are employed. Unlike in a SAR with constant PRI, the first samples of the received echoes correspond in a staggered SAR system to different slant ranges. Those echoes have therefore to be rearranged in a two-dimensional matrix with coordinates slant range and azimuth, associating each sample of the radar echo to the corresponding range. Raw data with gaps has then to be resampled to a uniformly spaced grid, as in [9].

The resampled raw data can then be focused using the approximated Omega-K algorithm. Fig. 5 shows the intensity of the focused data for the full scene of over 10000 km^2, where the strong returns of the ships can be observed. Fig. 6 (a) depicts a zoom around one of the large ships in the scene, for which the response extends in azimuth due to the presence of azimuth ambiguities. In addition to the ships, the range ambiguities of the ships are visible as sets of equally spaced lines parallel to the azimuth directions. Fig. 6 (b) depicts a zoom around the first order range ambiguity of the large ship of Fig. 6 (a).

If an automated detection algorithm based on a threshold, such as the one discussed in [12] were applied to the data, numerous false alarms would appear due to the ambiguities of the ships. Range ambiguities would, however, be no issue, if a finer PRI variation could be employed. In that case, in fact, their level would be well below the detection threshold. In our case, where the radar is limited in the selection of the PRIs, the range ambiguities of the ships can be identified based on their specific signature and expected distance from the ship. The specific signature of range ambiguity might even allow detecting and locating (large) ships outside the imaged swath, as long as sufficient power is received, e.g., through the sidelobes.

A total of 57 ships have been detected in the full scene, namely 10 small ships (ship length ≤ 25 m), 25 medium ships (25 m < ship length ≤ 150 m), and 22 large ships (ship length > 150 m).

IV. Validation with Ground Truth from AIS Data

The International Convention for the Safety of Life at Sea requires automatic identification system (AIS) transponders to be carried on all ships exceeding 300 tons engaged in international voyages, cargo ships of 500 tons and above not engaged in international voyages, and all passenger ships [13]. Communication losses in AIS systems can occur due to physical limitations of their components, such as very high frequency propagation losses or multipath signal reception effects. As a result, combining SAR and AIS data results in more effective ship monitoring by allowing the identification of illegal vessels that lack an AIS or vessels that do not broadcast AIS messages for technical reasons. The Maritime Security Lab at DLR's German Remote Sensing Data Center in Neustrelitz, Germany, has developed a possible approach for SAR-AIS data fusion for near real-time applications related to maritime situational awareness [13], [14]. Two different AIS datasets provided by Vesselfinder Limited and MarineTraffic have been used as ground truth to validate the effectiveness of the staggered ambiguous mode for ship monitoring. 247 positions associated to 13 ships were provided by Vesselfinder Limited, whereas 53 positions associated to 12 ships were provided by MarineTraffic. It is important to note that AIS transponders broadcast the position of the vessel at various time intervals ranging from two seconds for fast moving targets to three minutes for anchored vessels. AIS specifications for the vessel's size and type are not included in the MarineTraffic dataset, whereas the VesselFinder Limited dataset has this information for 8 out of 13 ships. Four of the 8 ships are fishing vessels, with the smallest being of 24 m × 7 m size, three ships are classified as cargo, and the largest ship is a tanker of 274 m × 48 m size.

AIS tracks have been projected into the focused SAR image of Fig. 5. Zooms around two detected fishing vessels are displayed in Fig. 7. It can be noticed that while the slant range position is consistent between the AIS and the SAR data, an azimuth shift appears. This is due to the so-called "train-off-the-track effect", i.e., the fact that a moving target induces an additional Doppler shift beyond that of a stationary target. Moving targets in focused SAR images therefore appear displaced in the azimuth direction from their actual geographical position by [15]:

$$\Delta_{az} = \frac{R_0 v_{r_{ship}}}{v_s}, \tag{3}$$

where R_0 is the ship slant range, $v_{r_{ship}}$ is the radial velocity of the ship, and v_s is the satellite velocity. Table III compares the radial velocity retrieved from AIS data to the radial velocity estimated from the azimuth shift observed on the SAR image compared to the AIS positions for the two ships depicted in Fig. 7, and we note a good agreement between the results.

Table III Comparison between the radial velocity retrieved from the AIS data and the radial velocity estimated from the azimuth shift observed on the SAR image compared to AIS positions.

Ship	**Radial velocity retrieved from the AIS data**	**Radial velocity estimated from the SAR image**
Small ship of 28 m × 6 m	1.51 m/s	1.56 m/s
Small ship of 24 m × 7 m	0.16 m/s	0.28 m/s

All ships that are present in both AIS datasets are correctly associated with the detected ships on the SAR image. Fig. 5 shows the detected ships presented in AIS datasets with diamond markers and the 43 ships detected solely in the TerraSAR-X image with green circle markers.

V. Conclusions

An experimental TerraSAR-X acquisition in staggered ambiguous mode imaging a ground swath of 110 km with 2.2 m azimuth resolution has been performed over the North Sea. Data have been processed and the detection results have been successfully validated using AIS data.

Due to some technological limitations of TerraSAR-X, a nonoptimal PRI sequence and chirp bandwidth had to be used for this experiment. While the use of a non-optimal PRI sequence has resulted in range ambiguities from ships still being above the detection threshold, their specific signature due to the PRI variation has still allowed for a clear discrimination between the ships and their ambiguities. Iterative subtraction of the impulse responses of each detected target (as in the CLEAN algorithm) or the use of an extended matching filter (that includes the ambiguities) could be useful and investigated in the future for the rejection of range ambiguities.

The experiment is significant because it has the potential to serve as a test bed for the validation of the ambiguous mode for ship monitoring. The exploitation of ambiguous modes can go beyond the monitoring of ships in open sea and be extended to other applications, such as deformation monitoring using permanent scatterers interferometry.

References

[1] A. Moreira, P. Prats-Iraola, M. Younis, G. Krieger, I. Hajnsek, and K. P. Papathanassiou, "A tutorial on synthetic aperture radar," *IEEE Geosci. Remote Sens. Mag.,* vol. 1, no. 1, pp. 6-43, March 2013.

[2] G. Di Martino and A. Iodice, "Coprime Synthetic Aperture Radar (CopSAR): A New Acquisition Mode for Maritime Surveillance," *IEEE Transactions on Geoscience and Remote Sensing*, vol. 53, no. 6, pp. 3110-3123, June 2015.

[3] G. Di Martino and A. Iodice, "Orthogonal Coprime Synthetic Aperture Radar," *IEEE Transactions on Geoscience and Remote Sensing*, vol. 55, no. 1, pp. 432-440, Jan. 2017.

[4] N. Ustalli; M. Villano, "High-Resolution Wide-Swath Ambiguous Synthetic Aperture Radar Modes for Ship Monitoring," *Remote Sensing*, vol. 14, no. 13, p. 3102, Jun. 2022.

[5] M. Villano, G. Krieger and A. Moreira, "Advanced spaceborne SAR systems with planar antenna," *2017 IEEE Radar Conference (RadarConf)*, Seattle, WA, USA, 2017, pp. 0152-0156.

[6] M. Cohen, A. Larkins, P. L. Semedo and G. Burbidge, "NovaSAR-S low cost spaceborne SAR payload design, development and deployment of a new benchmark in spaceborne radar," *2017 IEEE Radar Conference (RadarConf)*, Seattle, WA, USA, 2017, pp. 0903-0907.

[7] M. Villano, G. Krieger and A. Moreira, "Staggered SAR: High-Resolution Wide-Swath Imaging by Continuous PRI Variation," *IEEE Transactions on Geoscience and Remote Sensing*, vol. 52, no. 7, pp. 4462-4479, 1 July 2014.

[8] M. Villano, G. Krieger and A. Moreira, "A Novel Processing Strategy for Staggered SAR," *IEEE Geoscience and Remote Sensing Letters*, vol. 11, no. 11, pp. 1891-1895, Nov. 2014.

[9] M. Villano, G. Krieger, M. Jäger and A. Moreira, "Staggered SAR: Performance Analysis and Experiments with Real Data," *IEEE Transactions on Geoscience and Remote Sensing*, vol. 55, no. 11, pp. 6617-6638, Nov. 2017.

[10] M. Pinheiro et al., "Processing and Performance Analysis of NASA-ISRO SAR (NISAR) Staggered Data," *IGARSS 2019 - 2019 IEEE International Geoscience and Remote Sensing Symposium*, Yokohama, Japan, 2019, pp. 8374-8377.

[11] N. Ustalli and M. Villano, "Impact of Ambiguity Statistics on Information Retrieval for Conventional and Novel SAR Modes," *2020 IEEE Radar Conference (RadarConf20)*, Florence, Italy, 2020, pp. 1-6.

[12] N. Ustalli, G. Krieger and M. Villano, "A Low-Power, Ambiguous Synthetic Aperture Radar Concept for Continuous Ship Monitoring," *IEEE Journal of Selected Topics in Applied Earth Observations and Remote Sensing*, vol. 15, pp. 1244-1255, 2022.

[13] B. B. Smestad; B. E. Asbjørnslett, Ø. J. Rødseth, "Expanding the Possibilities of AIS Data with Heuristics," *TransNav Int. J. Mar. Navig. Saf. Sea Transp.* 2017, 11, 279–286.

[14] E. Schwarz, D. Krause, S. Voinov, H. Daedelow, S. Lehner, "Near real time applications for maritime situational awareness," *in Proceedings of the Fourth International Conference on Remote Sensing and Geoinformation of Environment (RSCY2016)*, Paphos, Cyprus, 4–8 April 2016.

[15] P. W. Vachon, R. A. English and J. Wolfe "Ship Signatures in RADARSAT-1 ScanSAR Narrow B Imagery Analysis with AIS Live Data," Technical Memorandum DRDC Ottawa. 52 pp 1-44.

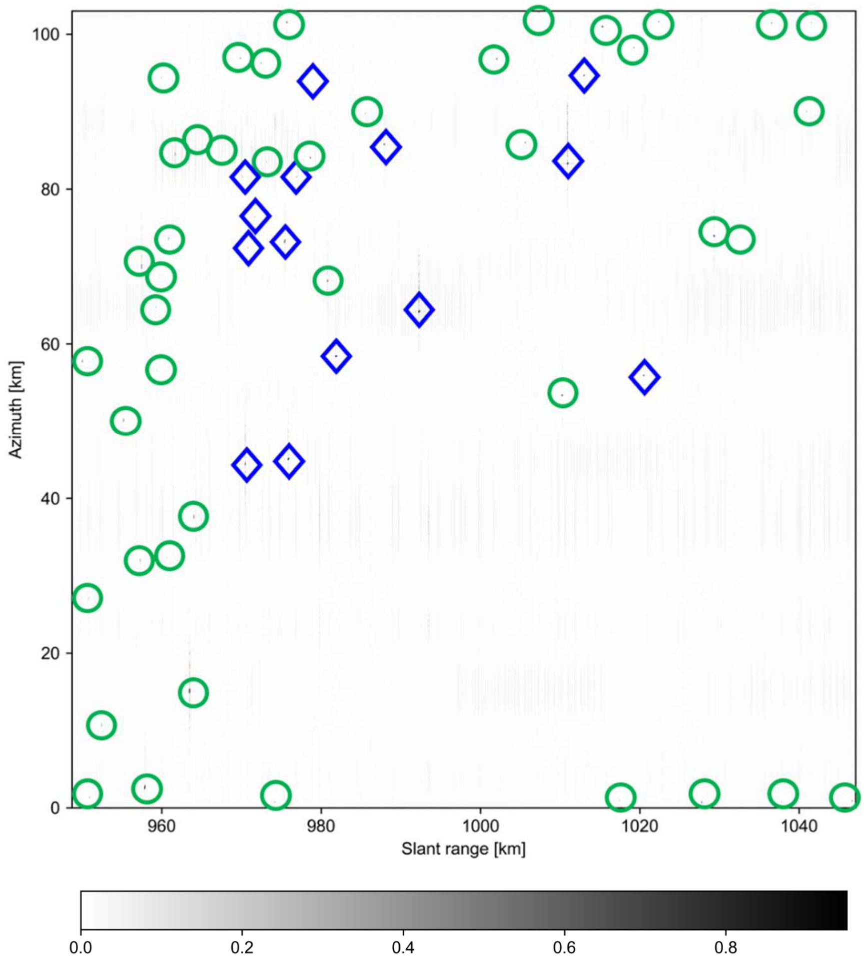

Fig. 5 Intensity of the focused image acquired by TerraSAR-X in staggered ambiguous mode over the full scene with superimposed the detected ships. Diamond markers highlight the detected ships that are presented in AIS datasets, and the green circle markers highlight the remaining 43 detected ships without AIS.

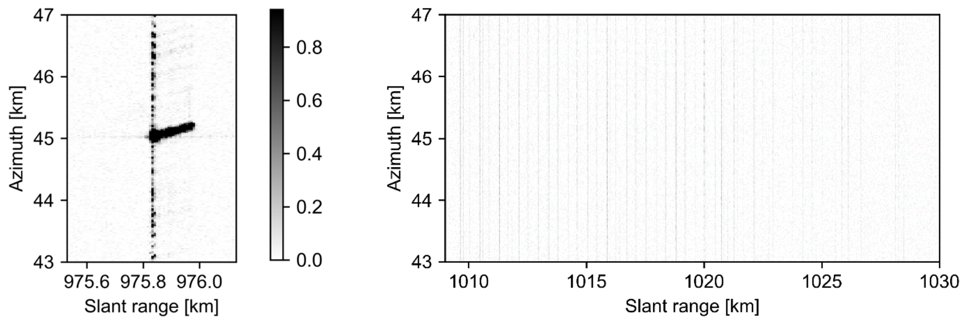

(a) (b)

Fig. 6 (a) Zoom around the large ship in Fig. 5 and its sidelobes (b) Zoom around its first-order range ambiguity of the large ship in Fig. 6 (a).

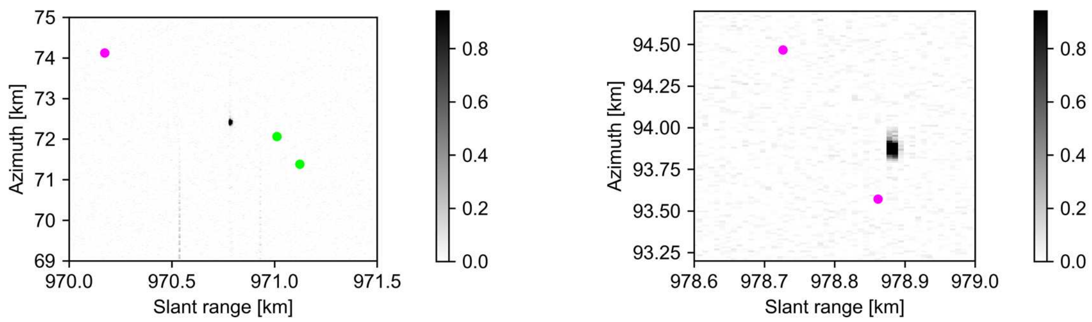

(a) (b)

Fig. 7 AIS tracks (green and purple points) overlaid to portions of the SAR image of Fig. 5 with ships. The purple and green portions of the AIS tracks correspond to the AIS points before and after the SAR acquisition, respectively (a) fishing vessel of 28 m × 6 m size with radial velocity of 1.15 m/s and azimuth shift of 192 m; (b) fishing vessel of 24 m × 7 m size with radial velocity of 0.16 m/s and azimuth shift of 21 m.